

# Zeeman effect of atomic uranium in the high lying odd levels measured by laser induced fluorescence spectroscopy

M. Oba<sup>1,a</sup>, K. Akaoka<sup>2</sup>, M. Miyabe<sup>1</sup>, and I. Wakaida<sup>1</sup><sup>1</sup> Tokai Research Establishment, Japan Atomic Energy Research Institute, Tokai-mura, Ibaraki-ken 319-1195, Japan<sup>2</sup> Kansai Research Establishment, Japan Atomic Energy Research Institute, 8-1, Umemi-dai, Kizuchō, Soraku-gun, Kyoto-hu 619-0215, Japan

Received 27 July 1999 and Received in final form 30 November 1999

**Abstract.** We measured Zeeman effect of atomic uranium spectra using laser induced fluorescence spectroscopy, and derived the  $J$ -value and  $g$ -factor of the second step levels.  $J$ -values and  $g$ -factors of high lying odd levels could be obtained. These data, especially the  $g$ -factors, have almost been unknown so far. We could verify our method which can be useful to measure  $J$ -values and  $g$ -factors of high lying levels of complex atoms like uranium.

**PACS.** 31.30.Gs Hyperfine interactions and isotope effects, Jahn-Teller effect – 32.30.Jc Visible and ultraviolet spectra – 32.60.+i Zeeman and Stark effects

## 1 Introduction

Spectroscopic parameters such as angular momenta  $J$ -values, Landé  $g$ -factors, radiative lifetime, transition probability, etc. of atoms are required in the analysis of the atomic structure, ionization spectroscopy and its applications. Measurement of Zeeman effect has been used for measurement of  $J$ -values and  $g$ -factors. Whereas such parameters of low-lying levels have been surveyed widely, fewer measurements have been taken for high-lying levels, in particular for heavy elements like actinides. As for uranium, sufficient data has not been obtained. Previous efforts have yielded  $J$ -values and  $g$ -factors of atomic uranium by measurement of Zeeman effect using hollow-cathode discharge with a strong magnetic field of greater than 1 tesla (T) and numerous data could be obtained [1,2]. However many levels remain unknown because, in addition to the complex atomic structure, its large  $J$ -value results in a complex Zeeman pattern. Therefore it is difficult to analyze their data due to low resolution of the hollow-cathode discharge. Some research groups measured  $J$ -values of high lying energy levels at around 4 eV by multi step laser photo-ionization method. They used the electric dipole selection rule. However,  $g$ -factors cannot be determined by these methods and the region of determined  $J$ -values were  $J = 5$  and  $J = 6$  [3–5]. Langlois *et al.* measured Zeeman effect of atomic uranium using optical galvanic detection in a hollow-cathode lamp and ring dye laser only for the first step levels [6]. Despite the many works provided [7], many unknown levels still exist.

Atomic beam laser spectroscopy is one of the most efficient methods in the high resolution spectroscopy, therefore it is useful especially for complex atoms like uranium. We measured the Zeeman effect of atomic uranium by high resolution atomic beam laser induced fluorescence spectroscopy in a magnetic field using two ring dye lasers, and obtained the  $J$ -values and  $g$ -factors of high lying odd levels around 4 eV. The region of determinable  $J$ -values is from  $J = 3$  to  $J = 8$ . In this paper, we report the measurement technique of  $J$ -values and  $g$ -factors of the high lying odd levels of atomic uranium.

## 2 Experiment

### 2.1 Experimental setup

Figure 1 shows the experimental setup. Two actively frequency stabilized single-longitudinal mode ring dye lasers pumped by Ar<sup>+</sup> lasers were used to excite atomic uranium to the high lying odd levels. One of them is for the first step excitation (Coherent CR699-21), and the other is for the second step excitation (Coherent CR699-29). Two laser beams are coupled by a beam splitter cube. The dyes used in this experiment were R6G or DCM. Wavelength of the laser for second-step excitation is monitored by temperature controlled confocal etalon whose free spectral range (FSR) is 750 MHz or 150 MHz, as the scanning marker.

Natural uranium metal piece with the <sup>238</sup>U isotope abundance of 99% was used. The isotope <sup>235</sup>U with the abundance of lower than 1%, which has a hyperfine structure can be considered negligible. Uranium atomic beam

---

<sup>a</sup> e-mail: oba@analchem.tokai.jaeri.go.jp

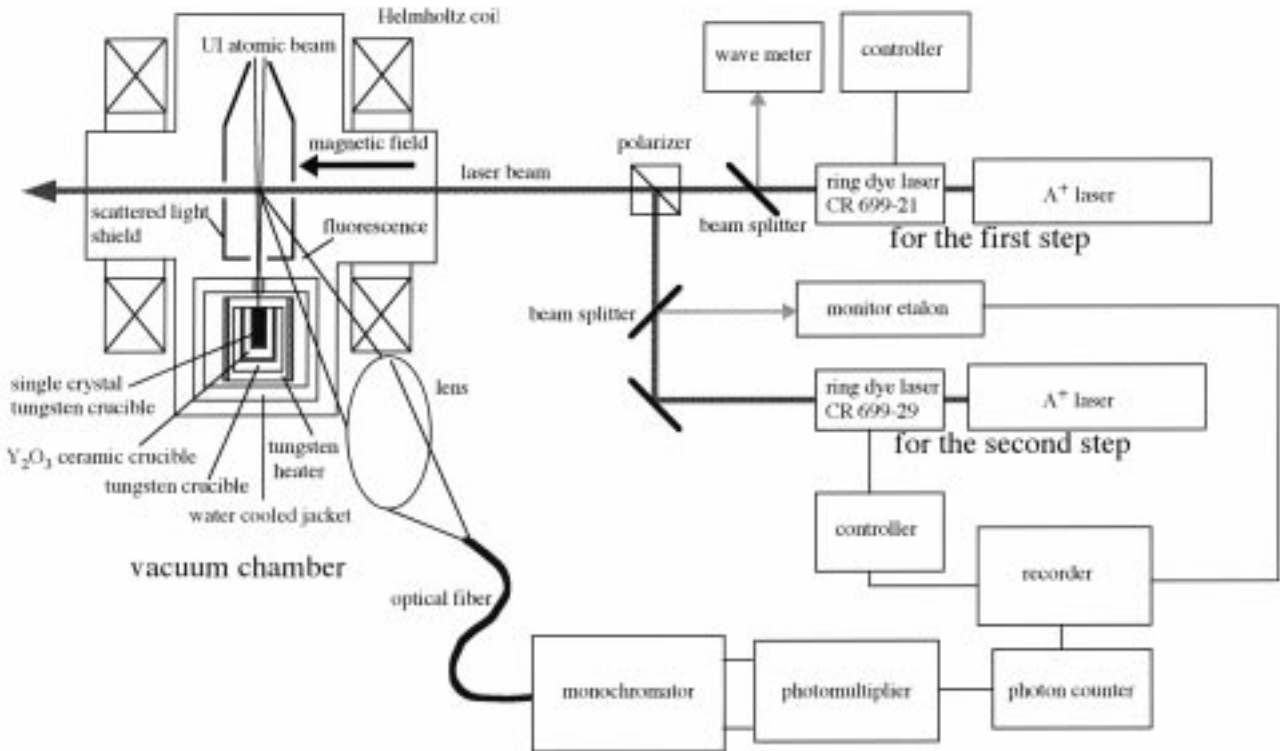


Fig. 1. Experimental setup.

is generated in the vacuum chamber by an oven. Though the electron beam evaporator can produce much higher density atomic beams, we did not use the electron beam evaporator, because of its vapor pressure instability. However, since high temperature liquid uranium corrodes many kinds of materials used for the crucible, a single crystal tungsten crucible, with the size of 4 mm (outside diameter)  $\times$  10 mm (long), 2 mm (inside diameter)  $\times$  8 mm (depth), was used. A threefold crucible was used to prevent the liquid uranium from flowing out. The uranium sample piece is set into the single crystal tungsten crucible, and this single crystal tungsten crucible is set into a  $Y_2O_3$  ceramic crucible and subsequently set into a polycrystalline tungsten crucible. The sample is heated to 1800 °C by the tungsten mesh heater, and the vapor is collimated by a 2 mm-diameter hole in order to reduce the Doppler broadening. Scattered light from the heater is so bright that scattered light shields and dumpers are required around the interaction region.

The laser beam crosses the uranium atomic beam perpendicularly and thus fluorescence is radiated from the atoms. Radiated fluorescence is fed into an optical fiber by a lens with an efficiency of 3% in the solid angle of the whole radiation direction. Fluorescence signal through the fiber is entered into the monochromator to reduce the radiation noise from the heater. Fluorescence with a different wavelength from that of the laser is selected by the monochromator to cut the scattered laser light noise. Fluorescence signal is detected by a photomultiplier cooled by Peltier element, and converted to electrical pulse signal, and then the pulses are counted by a photon counter.

A magnetic field is generated by a Helmholtz coil with the radius of 350 mm which is much larger than the interaction region of 2 mm-diameter and magnetic field is applied homogeneously with the fluctuation within 0.2% in the interaction region. The maximum field strength is  $6.90 \times 10^{-2}$  T that is high enough to observe Zeeman split spectral components separately, and low enough to neglect the nonlinear effects such as Paschen-Back effect. As the magnetic field's direction is the same as the laser beam's propagation direction, only the circular polarized transition can be observed.

## 2.2 Principle of J-value analysis

Figure 2 shows how to derive the  $J$ -values and  $g$ -factors from the experimental data. The first laser frequency is fixed to the one of the first excited Zeeman split components by the ring dye laser controller, then the second laser frequency is scanned around the second excited level. The  $J$ -value of the first excited level is assumed to be known as  $J_1$ . An example will be given in the case of the  $J$ -value difference  $\Delta J (= J_2 - J_1) = -1$ . At first, the first laser frequency is fixed to the component with the magnetic quantum number  $m_1 = J_1$  of the first excited level, and then only one spectral component ( $\Delta m = m_2 - m_1 = -1$ ) can be observed in the second step excitation. Next, the first laser frequency is fixed to the component of  $m_1 = J_1 - 1$ , then only one component can be observed again. Subsequently, the first laser frequency is fixed to the component of  $m_1 = J_1 - 2$ , then two spectral components can

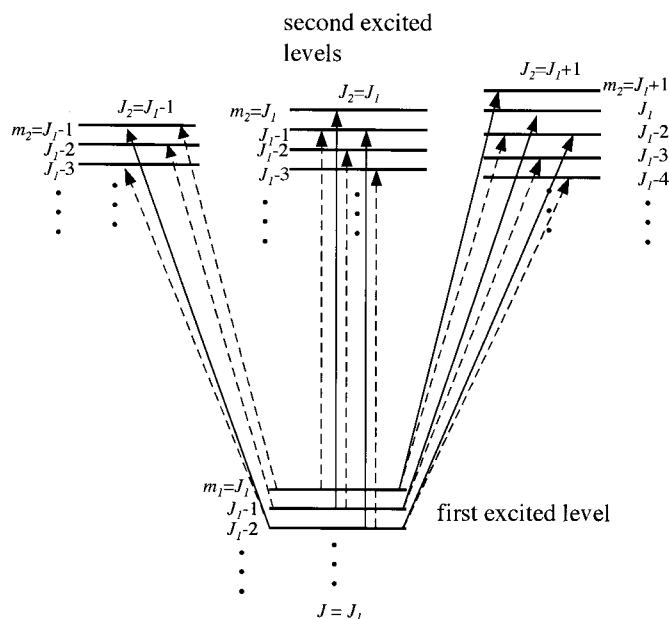


**Fig. 2.** Transition between Zeeman split sublevels and the circular polarized transition scheme, (—) for the  $\Delta m = +1$  transition, (---) for the  $\Delta m = -1$  transition.

**Table 1.** Relation between the number of observed spectrum and  $\Delta J$ ;  $m_1$  magnetic quantum number of the first excited sublevel,  $J_1$ :  $J$ -value of the lower level,  $J_2$ :  $J$ -value of the upper level.

$\Delta J (= J_2 - J_1)$ \ from $m_1$	$m_1 = J_1$ (or $-J_1$ )	$m_1 = J_1 - 1$ (or $-J_1 + 1$ )	$m_1 = J_1 - 2$ (or $-J_1 + 2$ )
+1	2	2	2
0	1	2	2
-1	1	1	2

be observed ( $\Delta m = -1$  and  $\Delta m = +1$ ). There is no need to measure all Zeeman spectral lines. It is adequate to only measure with respect to three transitions of them (components excited from  $m_1 = J_1, J_1 - 1, J_1 - 2$ ). Same process is applied to the other transitions such as  $J_1 \rightarrow J_2 (= J_1)$  and  $J_1 \rightarrow J_2 (= J_1 + 1)$ . Table 1 shows the relation between  $\Delta J$  and the number of observed Zeeman split spectral components. If the  $J$ -value of the first excited level is known then the  $J$ -value of the second excited level can be obtained. In principle,  $J$ -values and  $g$ -factors can be derived for all possible transitions. Since start levels are the ground state at  $0 \text{ cm}^{-1}$  ( $J = 6$ ) and metastable state at  $620 \text{ cm}^{-1}$  ( $J = 5$ ),  $J$ -value of the possible first excited levels are from  $J_1 = 4$  to  $J_1 = 7$  and that of the second excited levels are from  $J_2 = 3$  to  $J_2 = 8$ .

### 2.3 $g$ -factor analysis

The  $g$ -factor can be derived from the splitting interval of the spectral peaks and the applied magnetic field strength

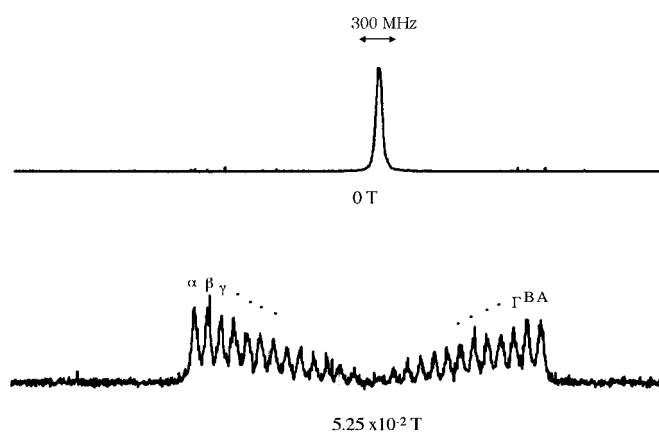


**Fig. 3.** Zeeman split pattern of the first step  $0\text{--}16\,900 \text{ cm}^{-1}$ .

using the following equation

$$\Delta E_m = g\mu_B H \delta m \quad (1)$$

where the  $\Delta E_m$  is the energy interval of the split levels,  $g$  is the Landé  $g$ -factor,  $\mu_B$  is the Bohr magneton,  $H$  is the magnetic field, and  $\delta m$  is the interval of the magnetic quantum number of the split sublevel. In the circular polarized transition  $\delta m = \pm 2$  ( $\Delta m = +1$  and  $\Delta m = -1$ ). The sign ( $\pm$ ) which depends on the sign of the  $g$ -factor, can be determined by assignment of the line component to the corresponding transition. To assign line components, relative intensity of each component is calculated by the squares of the  $3j$ -symbols [8]. The determined  $J$ -value can be confirmed by this calculated relative intensity of each component due to the difference of the relative intensity in the case of  $\Delta J = -1, 0, +1$ .

## 3 Results

Figure 3 shows Zeeman pattern of the first step transition from  $0 \text{ cm}^{-1}$  to  $16\,900 \text{ cm}^{-1}$  with magnetic field of  $5.25 \times 10^{-2} \text{ T}$ . The measured Doppler width was  $50 \text{ MHz}$ . As the  $J$ -values of the  $0 \text{ cm}^{-1}$  and  $16\,900 \text{ cm}^{-1}$  are known as  $J = 6$  and  $J = 7$  respectively, the number of Zeeman components are 26 for the circular polarized transition. The first component  $\alpha$  from the left of the Zeeman split component is the transition from  $m_1 = -6$  of the  $0 \text{ cm}^{-1}$  to the  $m_2 = -7$  of the  $16\,900 \text{ cm}^{-1}$ , and second component  $\beta$  is the transition from  $m_1 = -5$  to  $m_2 = -6$ , and so on.

Figure 4 shows the example of the observed second step Zeeman split spectra excited from the first excited level of  $16\,900 \text{ cm}^{-1}$  to  $34\,128 \text{ cm}^{-1}$  with the magnetic field of  $6.90 \times 10^{-2} \text{ T}$ . Figures 4a–4c show the transition from the  $\alpha$ ,  $\beta$  and  $\gamma$  indicated in Figure 3 respectively. The number of the observed Zeeman components excited from the  $\alpha$  that is the first transition to  $m_1 = -7$ , is one, and that from both  $\beta$  and  $\gamma$  are two. As seen in Table 1, relation of the  $J$ -value between  $16\,900 \text{ cm}^{-1}$  and  $34\,128 \text{ cm}^{-1}$  must be  $\Delta J = 0$ , therefore  $J$ -value of  $34\,128 \text{ cm}^{-1}$  is assigned as  $J = 7$ , that was disagreed with a previous work by Miron *et al.* [4]. They determined as  $J = 6$ .

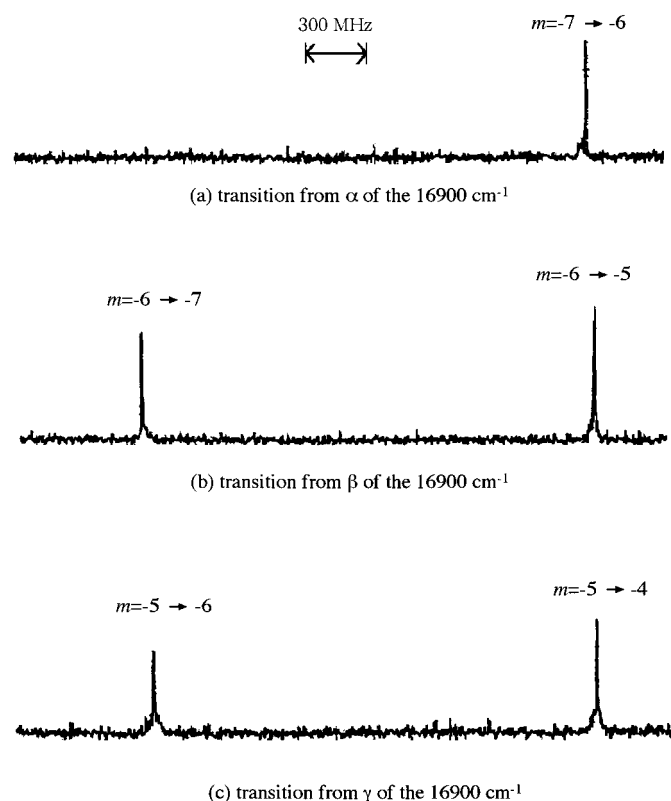


**Fig. 4.** Zeeman split spectrum of the second step from  $16900\text{ cm}^{-1}$  to  $34128\text{ cm}^{-1}$  magnetic field  $6.90 \times 10^{-2}\text{ T}$ , (a) transition from  $\alpha$  of the  $16900\text{ cm}^{-1}$ , (b) transition from  $\beta$  of the  $16900\text{ cm}^{-1}$ , (c) transition from  $\gamma$  of the  $16900\text{ cm}^{-1}$ .

In our measurement, a two-photon absorption or level crossing with a closed line, which cause miscounting of the spectral components, could be considered as the cause of this discrepancy. However, as the laser power density was lower than  $10\text{ W/cm}^2$ , the two-photon absorption should not have occurred, and since closed levels near the  $34128\text{ cm}^{-1}$  excited from  $16900\text{ cm}^{-1}$  could not be observed, level crossing should not occur. They determined a  $J$ -value of  $34128\text{ cm}^{-1}$  by observing the decay to  $10051\text{ cm}^{-1}$  whose  $J$ -value has been known as  $J = 5$ . However another decay transition might be observed, for example the transition from  $34128\text{ cm}^{-1}$  to  $10051\text{ cm}^{-1}$  is close to that from  $24066\text{ cm}^{-1}$  to  $0\text{ cm}^{-1}$  within  $0.2\text{ nm}$  difference in their wavelength [7] which is smaller than the accuracy of their monochromator described in their paper as  $0.3\text{ nm}$ . The latter transition might be observed in their measurement. Observed intensity ratio of the transition from  $m_1 = -5$  of the  $16900\text{ cm}^{-1}$  to  $m_2 = -6$  and  $m_2 = -4$  of the  $34128\text{ cm}^{-1}$  was 3:4. The calculated intensity ratio using  $3j$ -symbol is 1:66 in the case of  $\Delta J = -1$ , while 13:18 in the case of  $\Delta J = 0$ . This result seems to indicate  $\Delta J = 0$  rather than  $\Delta J = -1$ . Furthermore, Miyabe measured the  $J$ -value of this level by the dipole selection rule between this level and known autoionization levels, and his result agreed with ours [9].

Since the interval of the Zeeman component was  $2320\text{ MHz}$  at a magnetic field of  $6.90 \times 10^2\text{ T}$ , the  $g$ -factor could be obtained as 1.20. The line width of the lasers is smaller than  $1\text{ MHz}$  that is typical value of ring dye laser. However, the laser frequency fluctuation measured by temperature controlled spectrum analyzer, was  $20\text{ MHz}$ . The interval value is typically  $2\text{ GHz}$  and the accuracy of the  $g$ -factors could be estimated as 1%. Linear fit of the interval *versus* the magnetic field could not be measured because of insufficient resolution at the low magnetic field due to so many components. Therefore this systematic error was estimated by other elements such as gadolinium, and the result showed the systematic error within 1%.

Two closed levels were observed around the  $33046\text{ cm}^{-1}$  ( $33045.8\text{ cm}^{-1}$  and  $33046.1\text{ cm}^{-1}$  whose  $J$ -values were determined as 5 and 7, and  $g$ -factors were obtained as 1.11 and 1.15 respectively) excited from  $16505\text{ cm}^{-1}$  whose  $J$ -value is 6, with the interval of  $8\text{ GHz}$ . Using the transition selection rule, absolute laser wavelength must be given within an accuracy of  $0.2\text{ cm}^{-1}$ . If the line width of the laser is several GHz, then these levels cannot be distinguished. Even in such a case, our method enables us to observe them separately.

## 4 Summary

We suggest the method of  $J$ -values and  $g$ -factors measurement lying in the high odd levels of the atomic uranium by the Zeeman effect using atomic beam laser induced fluorescence spectroscopy, and verified the effectiveness of this method. The  $J$ -values from  $J = 3$  to  $J = 8$  and  $g$ -factors of the high lying odd levels can be obtained by our measurement technique. We could measure for the closed levels whose spectral interval is  $8\text{ GHz}$  at around  $33046\text{ cm}^{-1}$ . Disagreement of the  $J$ -value with the previous work was found out at the  $34128\text{ cm}^{-1}$  at which our result indicated  $J = 7$ .

The work was performed under the contract with the Atomic Energy Bureaus of Science and Technology Agency of Japan.

## References

1. J. Blase, L.J. Radziemski Jr, *J. Opt. Soc. Am.* **66**, 644 (1976).
2. L.J. Radziemski Jr *et al.*, *J. Opt. Soc. Am.* **61**, 1538 (1971).
3. L.R. Carlson *et al.*, *J. Opt. Soc. Am.* **66**, 846 (1976).
4. E. Miron *et al.*, *J. Opt. Soc. Am.* **69**, 256 (1979).
5. V.K. Mago *et al.*, *J. Phys. B* **20**, 6021 (1987).
6. E. Langlois, J.-M. Gagne, *J. Opt. Soc. Am. B* **4**, 1222 (1987).
7. *Crosswhite: Gmelin Handbook of Inorganic Chemistry*; Uranium, Suppl. Vol. **A5** (Berlin, Heidelberg, New York, Springer, 1982).
8. I.I. Sobel'man, *Introduction to the Theory of Atomic Spectra* (Oxford, New York, Toronto, Sydney, Braunschweig, Pergamon Press, 1972), Sect. 31.
9. M. Miyabe, private communication.